

SUPPLEMENTARY MATERIAL

SUPPLEMENTARY EXPERIMENTAL PROCEDURES

Subcloning and Purification

Most constructs were cloned into pET28 (Novagen) for expression studies except Msps TOG1-2 (1-505), MAST TOG1-TOGL1 (1-538), human EB1 full length (1-268), EB1₁₂₋₂₅₅, EB1₁₋₁₃₃, and CLIP-170₅₇₋₂₁₀ for which pGEX-2T or pGEX-6P2 (GE Healthcare) was used. CLIP-170₁₋₃₅₀ in pET19b (Novagen) was a gift from Holly Goodson. Proteins were expressed in BL21 DE3 cells under appropriate selection, induced with 100 μ M IPTG for 12 hr at 25° C. Cells were harvested, lysed in 25 mM Tris pH 8.0, 300 mM NaCl, 0.1% β -ME and 1 mM PMSF using a Microfluidizer (Microfluidics) and purified over either Ni²⁺-NTA (Qiagen) or glutathione sepharose (GE Healthcare) according to manufacturer's protocols. Where appropriate, the affinity tag was removed through addition of specific protease followed by ion exchange chromatography. Due to insolubility when expressed alone, Msps TOG1 was generated through plasmin treatment of Msps TOG1-2 (1-505) which cleaved between residues K241 and I242 (verified by N-terminal amino acid sequencing performed by the Yale Keck Center's Protein Sequencing Core).

Constructs for expression of +TIPs in *Drosophila* utilized a C-terminal EGFP fusion tag in the pMT-V5 HisA vector (Invitrogen). These constructs entailed EB1₁₋₁₉₁, CLIP-190₃₋₂₃₅ and Msps TOG1-4 (3-1175). Similar constructs were generated differing by the inclusion of a penultimate GCN4-leucine zipper motif followed by EGFP. For expression of rapamycin-sensitive constructs in HeLa cells, the rapamycin binding regions of mTOR (FRB domain: mTOR₂₀₂₁₋₂₁₁₃) and FKBP (2-108) were inserted into pEGFP-N (Invitrogen). Subsequently, human EB1₁₋₁₈₇, CLIP-170₃₋₂₁₀ and CLIP-170₁₂₉₋₃₅₀ were subcloned into each of the modified vectors. All mutants were generated by the Quickchange method (Stratagene).

Crystallization, Data Collection and Structure Determination

Msp_s TOG2 (residues 267-505) was subcloned into the vector pET28 (Novagen), transformed into B834 *E. coli*, grown as previously described at 37° C to an OD_{600nm} of 0.6, at which point the temperature was decreased to 20° C and 0.1 mM IPTG was added (Leahy et al., 1994). After a 16 hr induction period, cells were harvested, resuspended in lysis buffer (25 mM Tris pH 8.0, 300 mM NaCl 15 mM imidazole, 0.1 % β-ME, 5 mM L-methionine) and lysed using a microfluidizer (Microfluidics, Inc.). 2 mM PMSF was added and the lysate was clarified at 50,000 x g for 45 min. Supernatant was incubated with 15 ml Ni²⁺-NTA resin for 30 min at 4° C with rotation. Resin was collected by centrifugation, loaded onto a column and washed with 200 column volumes of lysis buffer. Protein was eluted with a 300 ml 15 to 300 mM imidazole gradient. Fractions containing SeMet-substituted Msp_s TOG2 protein were pooled, CaCl₂ was added to 2.5 mM and bovine α-Thrombin was added to a final concentration of 2.5 µg/ml at 4° C for 12 hr to remove the N-terminal hexahistidine tag. Protein was filtered over benzamidine sepharose, exchanged into 25 mM Tris pH 7.0, 0.1 % β-ME, 5 mM L-methionine, loaded onto a 10 ml SP Sepharose fast flow column (GE Healthcare) and eluted with a 300 ml 0-1 M NaCl gradient. Fractions containing protein were pooled, exchanged into 10 mM Tris pH 7.0, 200 mM NaCl, 0.1 % β-ME, 5 mM L-methionine, concentrated and stored at -80° C. SeMet-substituted Msp_s TOG2 was crystallized using the hanging drop vapor diffusion method at 20° C. 2 µl of protein at 15 mg/ml was added to 2 µl of mother liquor containing 2.25 M sodium malonate pH 7.0 and equilibrated over 1 ml of the mother liquor. SeMet-substituted Msp_s TOG2 crystallized in the space group C222₁ with one molecule in the asymmetric unit (a.s.u.). Crystals were transferred to 3.4 M Sodium malonate pH 7.0 and flash frozen in liquid nitrogen.

SeMet-substituted Stu2p TOG2 (residues 317-560) was expressed, purified and crystallized according to the protocol for SeMet-substituted Msp_s TOG2 except that the protein was stored in 10 mM Tris pH 7.0, 100 mM NaCl, 0.1 % β-ME, 5 mM L-methionine and crystallized using a mother liquor containing 27% PEG 4k, 100 mM sodium citrate pH 5.6, 200 mM ammonium acetate. Crystals belonged to the space group P2₁2₁2₁ with one molecule in the a.s.u. Crystals were transferred to mother liquor supplemented with 20% glycerol and flash frozen in liquid nitrogen.

SeMet-substituted EB1 (residues 12-133) was subcloned into pGEX-6P2 (GE Healthcare) creating an N-terminal GST fusion protein. Protein was expressed according to the procedure described for SeMet-substituted Msps TOG2. Cells were resuspended in lysis buffer (25 mM Tris pH 8.0, 300 mM NaCl, 0.1 % β -ME, 5 mM L-methionine) and lysed using a microfluidizer (Microfluidics, Inc.). 2 mM PMSF was added and the lysate was clarified at 36,000 x g for 45 min. Supernatant was incubated with 15 ml Glutathione-S-Sepharose (GE Healthcare) for 30 min. at 4° C with rotation. Resin was collected by centrifugation at 200 x g for 10 min., loaded onto a column and washed with 200 column volumes of lysis buffer. Protein was eluted with 50 ml of lysis buffer supplemented with 25 mM Glutathione pH 8.0. Prescission protease (GE Healthcare) was added to a final concentration of 2.5 μ g/ml to remove the N-terminal GST tag. Protein was exchanged into 25 mM Tris pH 7.0, 0.1 % β -ME, 5 mM L-methionine, loaded onto a 10 ml SP Sepharose fast flow column (GE Healthcare) and eluted with a 0 to 1 M NaCl gradient over 300 ml. Fractions containing protein were pooled, filtered over Glutathione-S-Sepharose (GE Healthcare), exchanged into 5 mM Tris pH 7.5, 200 mM NaCl, 0.1% β -ME, 5% glycerol, 5 mM L-methionine, concentrated and stored at -80° C. SeMet-substituted EB1 was crystallized using the hanging drop vapor diffusion method at 20° C. 2 μ l of protein at 20 mg/ml was added to 2 μ l of mother liquor containing 11.5% 2-propanol, 190 mM sodium citrate, 100 mM Hepes pH 7.0. Crystals were nucleated by streak-seeding. Crystals belonged to the space group P2₁ with two molecules in the a.s.u. Crystals were transferred to mother liquor supplemented with 30% glycerol and flash frozen in liquid nitrogen.

SeMet-substituted Bim1p (residues 1-124) was expressed, purified and crystallized according to the protocol for SeMet-substituted Msps TOG2 except that the protein was crystallized using a mother liquor containing 100 mM Tris pH 9.0, 200 mM lithium sulfate and 29% PEG 4k. Crystals belonged to the space group P2₁2₁2₁ with one molecule in the a.s.u. Crystals were transferred to mother liquor supplemented with 15% ethylene glycol and flash frozen in liquid nitrogen.

SeMet-substituted CLIP-170 Cap-Gly domain 1 Q124M (residues 57-128) was expressed, purified and crystallized according to the protocol for SeMet-substituted Msps TOG2 except

that the construct was subcloned into the vector pET15b (Novagen) and protein was stored in 10 mM Tris pH 7.0, 25 mM NaCl, 0.1% β -ME, 5 mM L-methionine and crystallized using a mother liquor containing 1.2 M sodium malonate, 100 mM glycine pH 9.0, 1.1 mM lanthanum chloride and nucleated by streak-seeding. Crystals belonged to the space group $P2_12_12$ with one molecule in the a.s.u. Crystals were transferred to mother liquor supplemented 25% ethylene glycol and flash frozen in liquid nitrogen.

Diffraction data were measured at the Lawrence Berkeley National Laboratory Advanced Light Source using beamlines 8.3.1 and 8.2.2 outfitted with ADSC 210 and 315 charge coupled device detectors respectively. Crystals were maintained at 100° K using a nitrogen cryo stream. Data were processed and scaled using DENZO and SCALEPACK (Otwinowski, 1997). Heavy atom searches were performed using an automated Patterson heavy atom search method in the CNS package (Brunger et al., 1998) and selenium peak anomalous wavelength data. MAD phasing used the selenium coordinates and the respective low energy remote wavelength as reference. Phases were improved by solvent flipping and density modification. Model building was done either manually with O (Jones et al., 1991) or initiated with ARP/wARP (Morris et al., 2002) and completed manually with O. Refinement was performed with the CNS package and monitored with a random 10% of the data used for cross-validation. Model refinement used the MLHL target function, torsion angle molecular dynamics simulated annealing (Rice and Brunger, 1994), B-factor refinement, and rebuilding in O with σ_A -weighted difference Fourier maps. The EB1 structure was initially refined to a resolution of 1.50 Å using the MLHL target function and then further refined to a resolution of 1.25 Å using the MLF target function and anisotropic B-factor refinement in Refmac5 (Murshudov et al., 1999). Figures were prepared with PyMOL (DeLano Scientific).

SUPPLEMENTARY FIGURE LEGENDS

Figure S1: Gel filtration analysis of tubulin : +TIP domain interaction

Gel filtration studies testing the interaction of +TIP domains with tubulin (A-M). Unless otherwise stated, traces are of +TIPs in the presence of tubulin and are colored as follows: Tubulin alone, black; +TIP domain(s) alone, red; +TIP and tubulin together, green. Plots indicate absorption at 280nm on the y-axis and elution volume in ml along the x-axis. A) Msps TOG1-2 cleaved with plasmin creating TOG1 and TOG2 in trans and run together. Inset: SDS-polyacrylamide Coomassie-stained gel; lanes 1) molecular weight markers, 2) Msps TOG1-2 uncut, 3) Msps TOG1-2 post plasmin cleavage. B) The Msps TOG1-2:tubulin complex analyzed over gel filtration (Shodex KW-803) by in-line dynamic light scattering. Experimentally determined complex masses are indicated. Relative concentrations of components: 12.5 μ M tubulin, 25 μ M Msps TOG1-2 (black curve); 25 μ M tubulin, 50 μ M Msps TOG1-2 (red curve); 50 μ M tubulin, 100 μ M Msps TOG1-2 (green curve). Experimentally determined reference masses (not shown): tubulin alone: 106 kDa (predicted: 110 kDa), Msps TOG1-2: 57 kDa (predicted: 57 kDa). Predicted mass for a 1:1 and a 1:2 binding ratio for MspsTOG1-2:tubulin is 167 and 277 kDa respectively. C) Msps TOG1-2 WT and mutants in the absence of tubulin (Msps TOG1-2 WT, green; Msps TOG1-2 W21E, light blue; Msps TOG1-2 W292E, dark blue; Msps TOG1-2 W21E W292E, pink. D) Stu2p TOG1. E) Stu2p TOG2. F) Stu2p TOG domains in the absence of tubulin: Stu2p TOG1, red; Stu2p TOG2, green; Stu2p TOG1 and TOG2 in trans together, dark blue. G) Stu2p TOG1 and TOG2 together in trans. H) Comparison of Stu2p – tubulin shifts: Stu2p TOG1 plus tubulin, red; Stu2p TOG2 plus tubulin, green; Stu2p TOG1 and TOG2 in trans plus tubulin, dark blue; tubulin alone, black. I) EB1₁₂₋₂₅₅. J) Bim1p₁₋₁₅₄. K) Bim1p₁₋₁₈₇. L) Bim1p₁₋₁₈₇-LZ. M) CLIP-170₅₇₋₂₁₀-GFP with TMR-doped tubulin, red (280nm), orange (550 nm); TMR-doped rhodamine tubulin alone, black (280 nm), grey (550 nm). All runs were performed on a Tricorn Superdex 200 10/30 gel filtration column except where noted.

Figure S2: TOG domain conservation

Sequence conservation of XMAP215 family TOG domains and mapping of the sequence to the solved structure. Sequence alignment of Msps (*Drosophila*), XMAP215 (*Xenopus*), Ch-TOG (Human), Zyg9 (*C. elegans*), Stu2p (*S. cerevisiae*), Dis1 (*S. pombe*), Alp14p (*S. pombe*), Mor1 (*A. thaliana*), CP224 (*D. discoideum*). Numbers after the protein name denote the TOG domain number. TOG domain 2 members are aligned above with 80% identity highlighted in green, 80% homology highlighted in yellow. Msps TOG domains 1, 3-5 are aligned below with 80% identity and homology shown in light blue and pink respectively, determined from multi-species alignments of that respective TOG domain number. Amino acids in TOG 1, 3-5 that correlate with 80% identity within their TOG group and also in TOG2 are highlighted in dark blue. Secondary structure of Msps and Stu2p TOG2 domains, based on their respective structures are indicated above the alignment. Side chain solvent accessibility of Msps TOG2, determined from the structure, is indicated below the alignment.

Figure S3: Homology analysis of microtubule and actin-binding CH domains

A) Sequence alignment of EB1 family member CH domains. Below the EB1 family is aligned two additional microtubule-binding CH domain families, the N-terminal CH domain from Ndc80p (of the kinetochore's Ndc80 complex) and the CH domain from CLAMP (Dougherty et al., 2005; Wei et al., 2007). Below the microtubule-binding CH domains are aligned actin-binding CH domains from solved structures. Respective PDB codes are appended to the protein name. Secondary structures of human EB1 and *S. cerevisiae* Bim1p are indicated above the alignment. Secondary structure of Hec1 and the actin binding CH domains are boxed in grey on their respective sequences. Regions of the CH1 and CH2 residues utilized for actin binding are boxed in red. Side chain solvent accessibility of human EB1, determined from the structure, is indicated below the alignment. Within the EB1 family, residues exhibiting 80% identity and 80% homology are highlighted in green and yellow respectively. Residues in the non-EB1 CH domain families that retain this conservation are similarly colored. Residues with 100% identity unique to the actin-binding CH domains are highlighted in orange. Results of CH domain cluster mutagenesis on the plus end tracking activity of EB1₁₋₁₈₇-LZ are indicated above the alignment: black font, no change in plus end tracking

activity; red font, no plus end tracking activity (diffuse cytosolic localization). Individual clusters are boxed. Species abbreviations are indicated below the alignment. B) $2F_o-F_c$ electron density map at 1.9 Å resolution of the Bim1p CH domain structure contoured at 1.0σ showing residues (magenta, also delineated in A) along the $\alpha 6$ - $\alpha 7$ loop that are 80% invariant across EB1 members but are not conserved in Bim1p. Insets indicate the relative orientation of Bim1p.

Figure S4: Structural comparison of actin-binding CH domains and the EB1 microtubule-binding CH domain.

A) Structure of the tandem CH1 and CH2 domains from plectin (pdb code 1MB8 (Garcia-Alvarez et al., 2003)) with helices represented in cylindrical form (CH1, light grey; CH2, dark grey). Images at right have been rotated 90° about the x-axis relative to the images at left. B) Relative orientation of two human EB1 CH domains after a least squares fit of each onto plectin CH1 and CH2. The pseudo 2-fold axis that relates the actin-binding CH domains is evident. C) Superimposition of plectin and human EB1 as in A and B. D) Actin-binding regions of plectin CH1 and CH2 colored red (as in Figure S3) with helices represented in cylindrical form (Mino et al., 1998). E) CPK representation of D. F) Conservation (80% identity in green, 80% homology in yellow) within the EB1 family with two EB1 CH domains oriented as in B in CPK representation.

Figure S5: Conserved sequence of Cap-Gly domains

Sequence alignment of Cap-Gly domains from CLIP-170 family members and additional tubulin-associated proteins. The first and second Cap-Gly from each CLIP-170 member is indicated by A and B respectively. Species abbreviations are listed below. Also included in the alignment are Cap-Gly domains from the p150Glued subunit of the dynactin complex, kinesin family members 13b (Human Gakin) and Klp73 (Drosophila), a Cap-Gly domain from *Anopheles gambiae*, and a Cap-Gly domain from CKAP1 (tubulin folding chaperone member). Positions of 80% identity and 80% homology are highlighted in green and yellow respectively. The secondary structure of the CLIP-170 Cap-Gly domain 1 is indicated above the alignment

as are the K98E, N99D and L124M mutations. Corresponding side chain solvent accessibility for the CLIP-170 Cap-Gly domain is indicated below the alignment. The loop insert present in F53F4.3 is highlighted in red.

Figure S6: The CLASP family of +TIP proteins likely shares a similar structural and biochemical mechanism to XMAP215 family members.

A) Domain organization of MAST, the *Drosophila* member of the CLASP family. The N-terminal TOG domain (TOG-1) is shown in green and central TOG-Like (TOGL) domains 1 and 2 in chartreuse. A final predicted domain of unknown structure is shown in brown first identified as the CLIP interaction domain (CLIP ID)(Akhmanova et al., 2001). B) Sequence alignment of the N-terminal TOG domain from CLASP family members. Species are indicated to the left. Below, Msps TOG2 is aligned and the corresponding secondary structural elements of Msps TOG2 are indicated. Positions of 80% identity and 80% homology are highlighted in red and orange respectively. Positions within Msps TOG2 that correlated with 80% identity within XMAP215 TOG2 members are shown in green as are the corresponding homologous residues in CLASP family members. C) Sequence alignment of tentative TOGL domains from CLASP family members. Helices predicted by the secondary structure prediction program PhDsec for *Drosophila* MAST are indicated above the alignments (Rost and Sander, 1993). 80% identity and 80% homology for CLASP family members are highlighted in red and orange respectively. Msps TOG2 intra-HEAT conserved loops are aligned below and residues conserved with CLASP members are highlighted in green for both protein families. Where appropriate, a composite TOG2 sequence is given where Msps TOG2 deviated from 80% identity within the XMAP215 family TOG2 alignment. Species utilized for alignments in B and C: Dm (*Drosophila melanogaster*), Dp (*Drosophila pseudoobscura*), Ag (*Anopheles gambiae*), Xl (*Xenopus laevis*), Hs (*Homo sapiens*), Bt (*Bos Taurus*). D) Polymerization of tubulin (12.5 μ M) determined via turbidity (y-axis, AU measured at 350 nm) over a 900 sec time span (x-axis) in the absence (black) and presence of MAST constructs TOG1-TOGL-1 (red), GST-TOG1-TOGL1 (green) and TOG1 (blue) (all +TIPs at 1 μ M respectively). A GST control had no effect on tubulin's polymerization as monitored by turbidity, and analysis of MAST constructs alone showed no increase in absorbance at 350nm

over time (data not shown). E) Analysis of TMR-labeled tubulin polymerized as in (D), fixed in glutaraldehyde and pelleted onto coverslips for imaging. Reactions were fixed at $t = 100$ and 300 sec in the presence or absence of +TIP constructs. Scale bar indicates $50 \mu\text{m}$.

SUPPLEMENTARY MOVIE LEGENDS

Movie S1: Mutation of the Cap-Gly tubulin binding site ablates microtubule plus end tracking

Video montage comparison of the microtubule plus end tracking competent construct CLIP-190₃₋₂₃₅-LZ (above) versus the corresponding GKNDG motif mutant: GEDDG (K98E, N99D) (below) that exhibits diffuse cytoplasmic localization and no plus end tracking activity in Drosophila S2 cells. The CLIP-190₃₋₂₃₅-LZ construct contains only the first Cap-Gly domain plus flanking regions from CLIP-190 and is artificially dimerized by fusion to the GCN4 leucine zipper motif. Movies were captured at a 2 sec frame interval.

Movie S2: Dimerization of the EB1 N-terminal region facilitates microtubule plus end tracking

Video montage comparison of Drosophila S2 cells transfected with monomeric (EB1₁₋₁₉₁, above) versus homodimeric (EB1₁₋₁₉₁-LZ, below) EB1 N-terminal regions. EB1₁₋₁₉₁ yields diffuse cytoplasmic localization whereas the homodimerized counterpart gives robust microtubule plus end tracking activity. The EB1₁₋₁₉₁ construct lacks the protein's native dimerization domain and is thus monomeric. Movies were captured at a 2 sec frame interval.

Movie S3: Dimerization of a single Cap-Gly domain facilitates microtubule plus end tracking

Video montage comparison of Drosophila S2 cells transfected with a single CLIP-190 Cap-Gly domain construct (CLIP-190₃₋₂₃₅, above) versus the artificially dimerized counterpart (CLIP-190₃₋₂₃₅-LZ, below). The monomeric construct yields diffuse cytoplasmic localization whereas the homodimerized counterpart localizes dynamically to the microtubule plus end. Movies were captured at a 2 sec frame interval.

Movie S4: Titrating the number of TOG domains controls microtubule affinity

Video montage comparison of *Drosophila* S2 cells transfected with constructs embodying either the first four TOG domains from Msps (above) or eight TOG domains created by artificially dimerizing Msps TOG1-4 with a leucine zipper motif (below). Msps TOG1-4 yields diffuse cytosolic localization whereas the artificially dimerized counterpart localized to microtubules. Full length Msps is monomeric and the plus end tracking activity is mediated through contributions by the five N-terminal TOG domains acting in concert with a conserved C-terminal domain. Frames were acquired at a 2 sec interval.

Movies S5A and S5B: Chemical dimerization of the EB1 N-terminal region dynamically induces microtubule plus end tracking

HeLa cells were dually transfected with EB1₁₋₁₈₅ N-terminal domain constructs fused to the rapamycin binding domains of FRB and FKBP. Both protein fusions give diffuse cytosolic localization in trans. However, upon treatment with 50 nM rapamycin, the fusion proteins become chemically dimerized and are dynamically recruited to the microtubule plus end. Addition of rapamycin after 1 min of acquisition is noted during the video as “+ Rapamycin”. Frames were acquired at a 2 sec interval in A, and a 3 sec interval in B. In movie S5B, a 144 sec segment of the video taken after rapamycin addition was removed due to refocusing.

Movie S6: Chemical dimerization of CLIP-170 Cap-Gly region 1 to Cap-Gly region 2 induces microtubule plus end tracking

HeLa cells were dually transfected with CLIP-170₃₋₂₁₀-FRB (containing Cap-Gly 1) and CLIP-170₁₂₉₋₃₅₀-FKBP (containing Cap-Gly 2). Initial localization of the constructs in trans is cytosolic and diffuse. After 1 min of acquisition, 50 nM rapamycin was added, noted by “+ rapamycin” in the video. Constructs become chemically dimerized and are

dynamically recruited to the microtubule plus end yielding robust microtubule plus end tracking behavior. Frames were acquired at a 2 sec interval.

Movie S7: Heterodimerization across +TIP families facilitates microtubule plus end tracking

To test if plus end tracking was conferred only by intra-family dimerization, HeLa cells were dually transfected with EB1₁₋₁₈₅-FRB and CLIP-170₃₋₂₁₀-FKBP. Initial localization of these constructs in trans is cytosolic and diffuse. After 1 minute of acquisition, 50 nM rapamycin was added at which point fusion proteins become chemically heterodimerized and are dynamically recruited to the microtubule plus end. Microtubule plus end tracking is evident albeit not as robust as in EB1 or CLIP-170 chemical dimerization experiments (Movies S5A-B and S6). The addition of rapamycin is denoted in the video by “+ Rapamycin”. Frames were acquired every 2 seconds.

SUPPLEMENTARY MATERIAL REFERENCES

- Akhmanova, A., Hoogenraad, C. C., Drabek, K., Stepanova, T., Dortland, B., Verkerk, T., Vermeulen, W., Burgering, B. M., De Zeeuw, C. I., Grosveld, F., and Galjart, N. (2001). Clasps are CLIP-115 and -170 associating proteins involved in the regional regulation of microtubule dynamics in motile fibroblasts. *Cell* *104*, 923-935.
- Brunger, A. T., Adams, P. D., Clore, G. M., DeLano, W. L., Gros, P., Grosse-Kunstleve, R. W., Jiang, J. S., Kuszewski, J., Nilges, M., Pannu, N. S., *et al.* (1998). Crystallography & NMR system: A new software suite for macromolecular structure determination. *Acta Crystallogr D Biol Crystallogr* *54*, 905-921.
- Dougherty, G. W., Adler, H. J., Rzadzinska, A., Gimona, M., Tomita, Y., Lattig, M. C., Merritt, R. C., Jr., and Kachar, B. (2005). CLAMP, a novel microtubule-associated protein with EB-type calponin homology. *Cell Motil Cytoskeleton* *62*, 141-156.
- Garcia-Alvarez, B., Bobkov, A., Sonnenberg, A., and de Pereda, J. M. (2003). Structural and functional analysis of the actin binding domain of plectin suggests alternative mechanisms for binding to F-actin and integrin beta4. *Structure* *11*, 615-625.
- Honnappa, S., Okhrimenko, O., Jaussi, R., Jawhari, H., Jelesarov, I., Winkler, F. K., and Steinmetz, M. O. (2006). Key interaction modes of dynamic +TIP networks. *Mol Cell* *23*, 663-671.
- Jones, T. A., Zou, J. Y., Cowan, S. W., and Kjeldgaard, M. (1991). Improved methods for building protein models in electron density maps and the location of errors in these models. *Acta Crystallogr A* *47 (Pt 2)*, 110-119.
- Leahy, D. J., Erickson, H. P., Aukhil, I., Joshi, P., and Hendrickson, W. A. (1994). Crystallization of a fragment of human fibronectin: introduction of methionine by site-directed mutagenesis to allow phasing via selenomethionine. *Proteins* *19*, 48-54.
- Li, S., Finley, J., Liu, Z. J., Qiu, S. H., Chen, H., Luan, C. H., Carson, M., Tsao, J., Johnson, D., Lin, G., *et al.* (2002). Crystal structure of the cytoskeleton-associated protein glycine-rich (CAP-Gly) domain. *J Biol Chem* *277*, 48596-48601.
- Mino, T., Yuasa, U., Nakamura, F., Naka, M., and Tanaka, T. (1998). Two distinct actin-binding sites of smooth muscle calponin. *Eur J Biochem* *251*, 262-268.
- Morris, R. J., Perrakis, A., and Lamzin, V. S. (2002). ARP/wARP's model-building algorithms. I. The main chain. *Acta Crystallogr D Biol Crystallogr* *58*, 968-975.
- Murshudov, G. N., Vagin, A. A., Lebedev, A., Wilson, K. S., and Dodson, E. J. (1999). Efficient anisotropic refinement of macromolecular structures using FFT. *Acta Crystallogr D Biol Crystallogr* *55*, 247-255.

Otwinowski, Z. a. M., W. (1997). Processing of X-ray diffraction data collected in oscillation mode. *Macromolecular Crystallography Pt a*, 307-362.

Rice, L. M., and Brunger, A. T. (1994). Torsion angle dynamics: reduced variable conformational sampling enhances crystallographic structure refinement. *Proteins 19*, 277-290.

Rost, B., and Sander, C. (1993). Prediction of protein secondary structure at better than 70% accuracy. *J Mol Biol 232*, 584-599.

Wei, R. R., Al-Bassam, J., and Harrison, S. C. (2007). The Ndc80/HEC1 complex is a contact point for kinetochore-microtubule attachment. *Nat Struct Mol Biol 14*, 54-59.

Figure S1

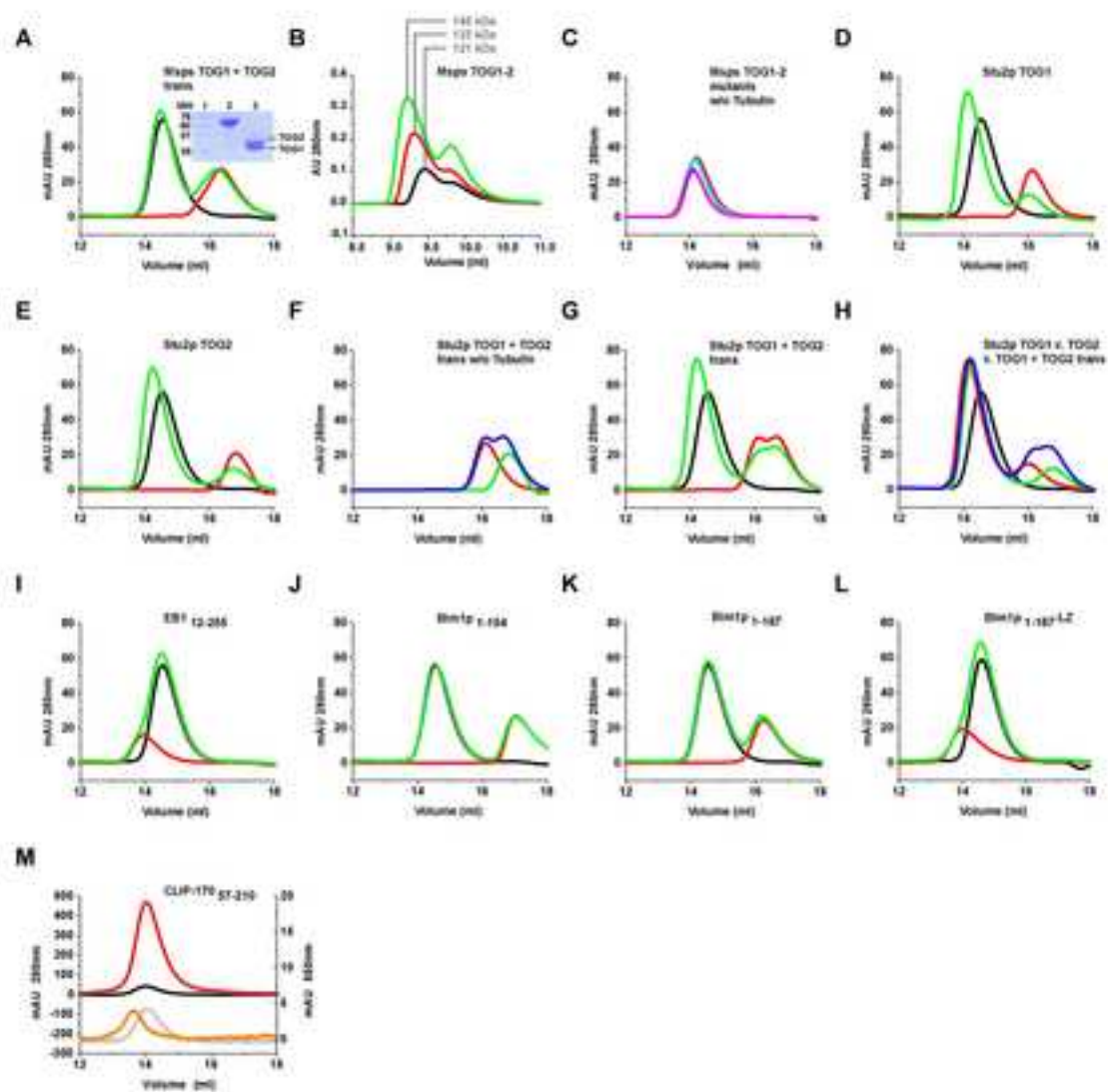


Figure S2

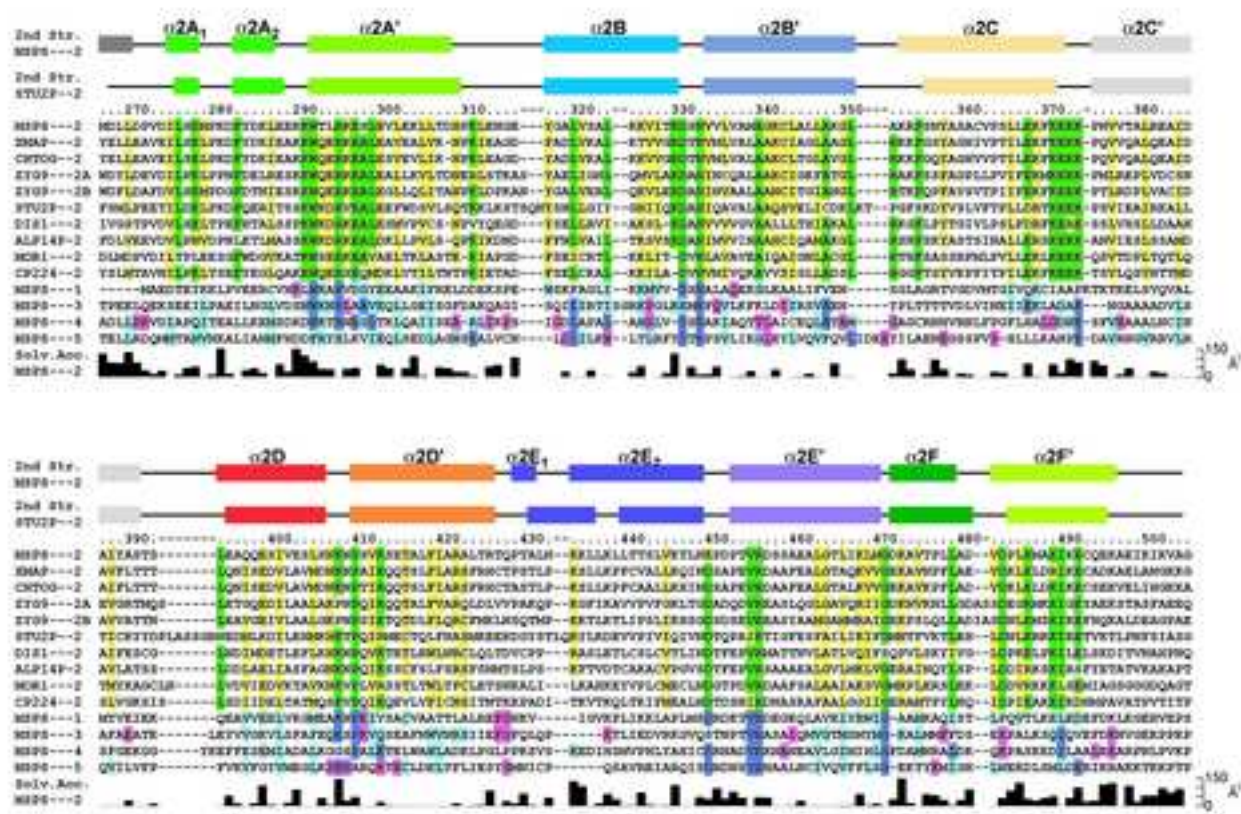


Figure S4

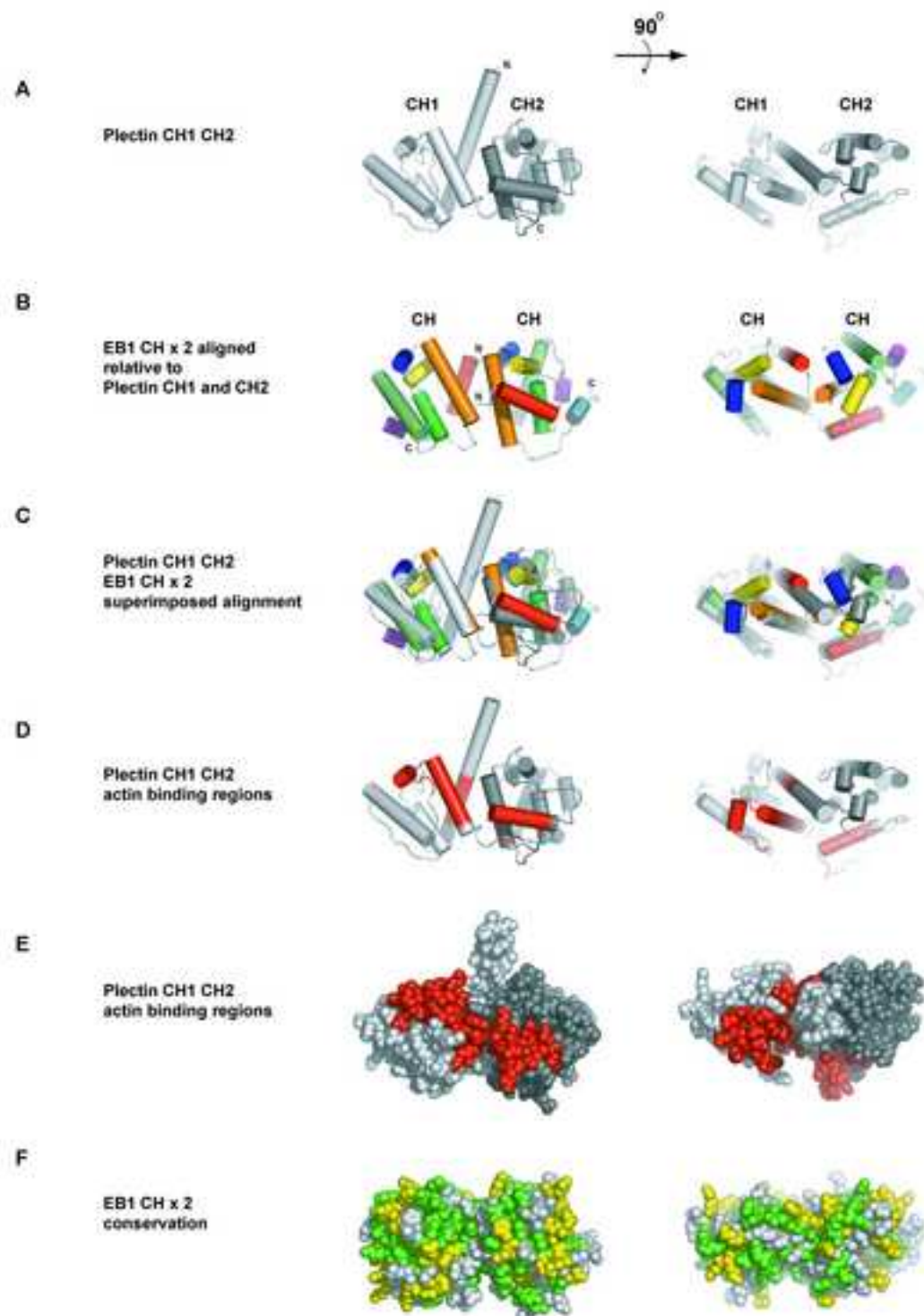


Figure S5

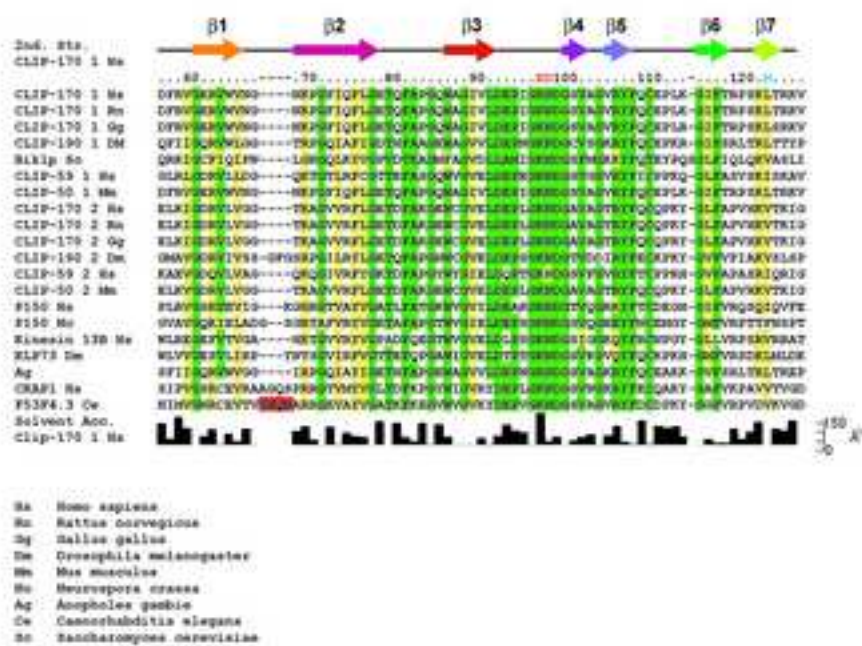


Figure S6

